Structural and electrical properties evolution in $Ba_{1-x}Sr_xRuO_3$ synthesized under high pressure

Jinggeng Zhao [a,b], Liuxiang Yang [a], Yong Yu [a], Fengying Li [a], Richeng Yu [a], Changqing Jin [a,*]

[a] Beijing National Laboratory for Condensed Matter Physics, Institute of Physics, Chinese Academy of Sciences, Beijing 100190, PR China
[b] Natural Science Research Center, Academy of Fundamental and Interdisciplinary Sciences, Harbin Institute of Technology, Harbin 150080, PR China

ABSTRACT

The 6H and 6M $Ba_{1-x}Sr_xRuO_3$ at $x \leqslant 0.6$ with the normal and distorted hexagonal $BaTiO_3$ structures were synthesized by using high-pressure and high-temperature method. It is found that the unit cell volume deviates from Vegard's law between 0.3 and 0.4 for the solid solutions due to the increasing distortion degree of crystal structure. With the increasing x, the electrical resistivity at the same temperature is increasing. With the substitution of Sr for Ba ion, the 6H $BaRuO_3$ transforms to a Fermi-liquid metal at $x = 0.25$ from the primal non-Fermi-liquid metal, and then becomes a semiconductor at low temperature when x is larger than 0.4.

© 2009 Elsevier Inc. All rights reserved.

1. Introduction

The oxide ruthenates have received growing attention for their unique physical properties. For example, Sr_2RuO_4, with the K_2NiF_4-type structure, is a superconductor of unconventional p-wave paring mechanism [1]. The alkaline-earth ruthenate $ARuO_3$ (A = Ca, Sr, and Ba) is an important system of oxide ruthenates [2]. $SrRuO_3$ and $CaRuO_3$ adopt the orthorhombic perovskite structure with the space group $Pnma$ [3,4]. There are three types of hexagonal perovskite-type $BaRuO_3$ reported, namely 9R, 4H, and 6H [5–7], where the number is the amount of BaO_3 layers in a unit cell, and the R and H denote the rhombohedral (space group: $R\text{-}3m$) and hexagonal (space group: $P6_3/mmc$) structures, respectively.

With the decreasing temperature, the 9R $BaRuO_3$ transforms to insulator-like from metallic behavior at about 110 K due to the pseudogap open [8,9]. It is of short-range antiferromagnetic order at high temperature, with the Néel point about 440 K [9,10]. The 4H $BaRuO_3$ is paramagnetic down to liquid helium temperature [8]. It is a normal Fermi-liquid metal. Recently, we have obtained the pure 6H $BaRuO_3$ at 5 GPa and 1000 °C [11], and found that it is an abnormal paramagnetic metal deviated from the Fermi-liquid behavior [11].

The chemical substitution of M cation for 1/3 Ru cation at ambient pressure can make the 9R $BaRuO_3$ transform to the $Ba_3MRu_2O_9$ compounds, where M = alkali metals, alkaline-earth

elements, 3d transition metals, and lanthanide elements. They adopt the normal or distorted hexagonal $BaTiO_3$ structures [12,13]. Longo et al. synthesized the $Ba_{1-x}Sr_xRuO_3$ solutions using high-pressure sintering at 1000 °C up to 9 GPa and indicated that both high pressure and chemical substitution can make $BaRuO_3$ transform to perovskite across the 4H and 6H forms from the primal 9R form [7]. However, the structural and physical properties of this series and the correlations between the RuO_6 polyhedron connections with their physics have not been available so far due to the difficulty to prepare single-phase samples.

In this paper, we successfully obtained the 6H $Ba_{1-x}Sr_xRuO_3$ series by using the high-pressure and high-temperature synthesis method and found that the solutions transform to the distorted hexagonal $BaTiO_3$ structure with the space group $C2/c$ at $x \geqslant 0.4$, which is different from the results in [7]. The structure of our 6M form is similar with that of the ambient-pressure phase of $SrIrO_3$ [14], so it is denoted to 6M. Fig. 1(a) and (b) show the schematic views of the 6H and 6M $Ba_{1-x}Sr_xRuO_3$, respectively. For the first time the structural detail based on Rietveld refinement, together with the systematic characterization of electrical properties of the 6H and 6M $Ba_{1-x}Sr_xRuO_3$ ($0.0 \leqslant x \leqslant 0.6$) was obtained.

2. Experimental

The ambient phases of $Ba_{1-x}Sr_xRuO_3$ were synthesized by using the method of conventional solid-state chemical reaction. The starting materials were barium and strontium carbonates
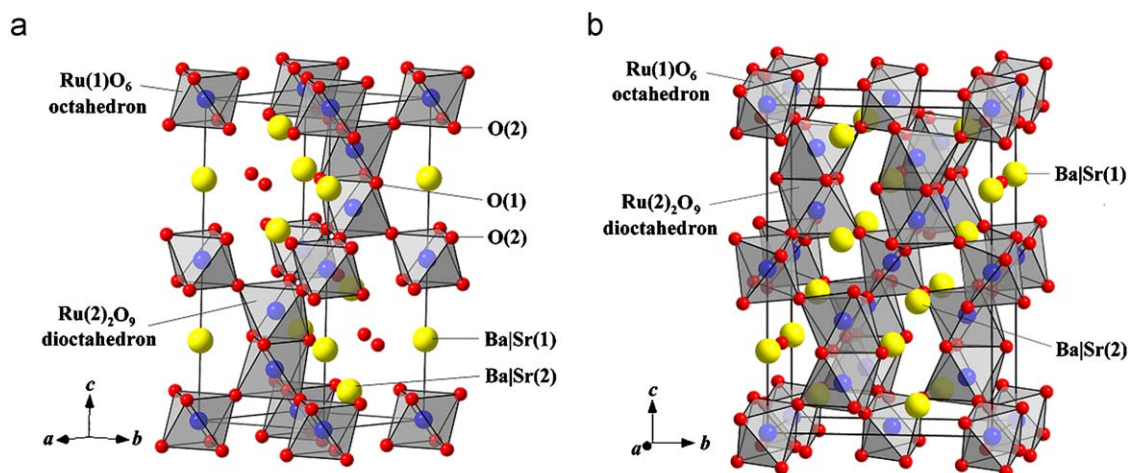
Fig. 1. The schematic views of the crystallographic forms of $Ba_{1-x}Sr_xRuO_3$: (a) 6H form and (b) 6M form. The RuO_6 octahedrons are represented by geometrical coordination (Ru at the center, O at corners). The unit cells are outlined.

(99.9% purity) and ruthenium metal (99.9% purity). Stoichiometric quantities of materials were mixed together, ground about 30 min in an agate mortar, and placed into an Al_2O_3 crucible. Then the powder was calcined for about 12 h at 1000 °C in air. The calcined powder was reground, pressed into a pellet at the pressure of 10 MPa, and sintered at 1100 °C for about 48 h in air with twice intermediate regrinding. The products were polycrystalline powder in black.

A conventional cubic-anvil type high-pressure facility was used to perform the high-pressure and high-temperature experiments. The ambient $Ba_{1-x}Sr_xRuO_3$ were pressed into pellets of 5.0 mm diameter, and then wrapped with gold foil to avoid contamination. The pellets were put into an h-BN sleeve which was in turn inserted into a graphite tube heater. Pyrophyllite was used as the pressure-transmitting medium. The treating process was carried out at 1.5–5.0 GPa and 1000 °C for about 30 min, followed by a quench from high temperature before releasing pressure with the rate about 0.6 GPa/min. The 6H $Ba_{1-x}Sr_xRuO_3$ ($0.0 \leqslant x \leqslant 0.3$) are obtained at 5.0 GPa, and the 6M phases are synthesized at 4.5 GPa ($x = 0.4$), 3.5 GPa ($x = 0.5$), and 1.5 GPa ($x = 0.6$).

The structures of our samples were checked by the powder X-ray diffraction (XRD) with $CuK\alpha$ radiation at room temperature, using a Rigaku diffractometer (MXP-AHP18). The experimental data for the $x = 0.0, 0.1, 0.2, 0.3, 0.6$ samples were collected in 2θ-steps of 0.02° and 3 s counting time in the range of 10°–120° and analyzed with Rietveld method by using the FullProf program [15]. The measurements of temperature dependences of electrical resistivity were performed by using the standard four-probe method with Ag paste contacts in the temperature range of 3–300 K on an Oxford Maglab.

3. Results and discussion

3.1. Crystal structure

Fig. 2(a) shows the observed and fitted XRD patterns of the 6H $Ba_{0.8}Sr_{0.2}RuO_3$. The XRD data are fitted with the $P6_3/mmc$ space group and analyzed with the Rietveld method. Table 1 lists the lattice parameters, atomic positional parameters, and conventional Rietveld R-factors for the 6H $Ba_{1-x}Sr_xRuO_3$ ($0.0 \leqslant x \leqslant 0.3$). The obtained R_p, R_{wp}, and R_{exp} factors indicate the good
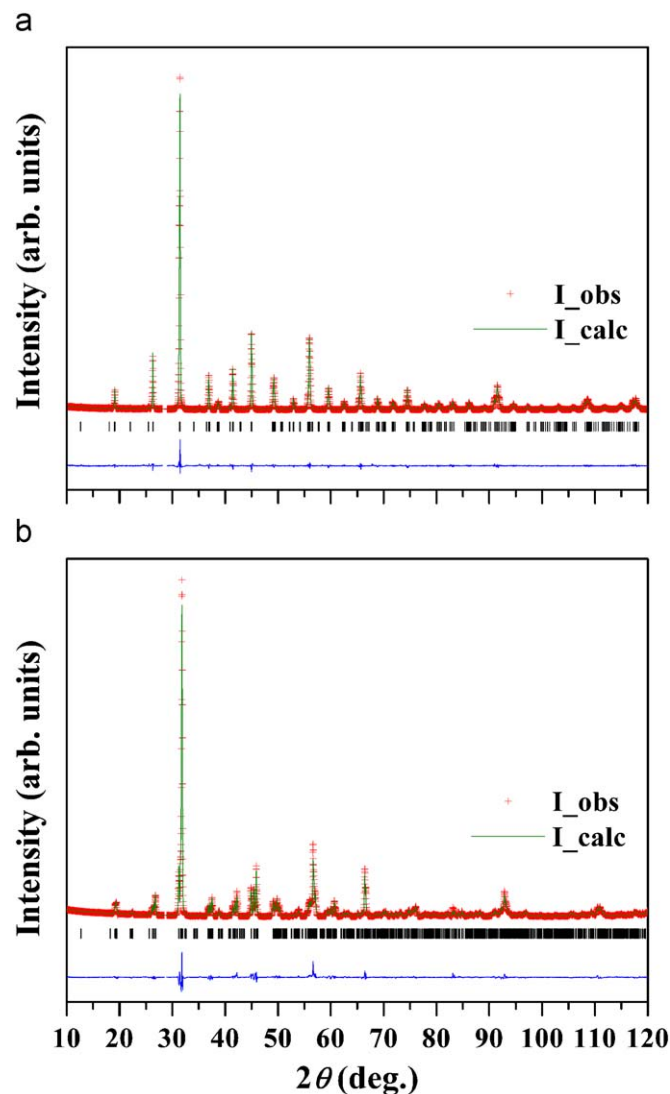
Fig. 2. The experimental (cross) and fitted (solid line) X-ray diffraction patterns for $Ba_{1-x}Sr_xRuO_3$: (a) the 6H $Ba_{0.8}Sr_{0.2}RuO_3$ and (b) the 6M $Ba_{0.4}Sr_{0.6}RuO_3$. The difference plots between observed and calculated patterns are shown at the bottom. The positions of the Bragg reflections are shown by the vertical lines.